



The Quantification of the Geological Strength Index (GSI): A Review

Fahmy O. Mohammed ¹ , Azealdeen S. Al-Jawadi ^{2*} , Iman M. Jaafar ³ , Colin Davie ⁴ 

¹ Department of Geology, College of Science, University of Sulaimani, Sulaimani, Iraq.

² Department of Mining Engineering, College of Petroleum and Mining Engineering, University of Mosul, Mosul, Iraq.

³ Department of Geology, College of Science, University of Basrah, Basrah, Iraq.

⁴ College of Civil Engineering and Geosciences-Newcastle University, UK.

Article information

Received: 24- Feb -2024

Revised: 25- Apr -2024

Accepted: 11- May -2024

Available online: 01- Apr – 2025

Keywords:

Geological Strength Index
Rock Quality Designation
Block Volume
Discontinuities
Rock Mass Classification

Correspondence:

Name: Azealdeen S. Al-Jawadi

Email:

azealdeenaljawadi@uomosul.edu.iq

ABSTRACT

The first Geological Strength Index (GSI) Chart was invented to classify rock mass properties. The GSI Chart developer assumes that qualified and skilled geologists or engineering geologists would evaluate and record the rock mass properties. Without a robust geological background and field experience, many researchers misuse the GSI charts. Due to the abnormal increase in GSI charts used in the recent decade, the update was necessary to eliminate visualization and assumption problems in GSI charts. The correlation between the quantified GSI charts was fair to reduce the uncertainty in estimating the rock strength properties. Many GSI charts were developed or updated to be quantified rather than visualized charts, which have become more specific and universal. The GSI Chart was modified by including additional parameters such as joint condition, rock quality designation RQD, volumetric joint count (Jv), and block volume (Vb). The modified GSI charts facilitate more practical use and reduce error. However, field observation and visualization are still essential for rock strength property estimation, particularly in the geomechanical classification of the rock mass. Some modifications add too much complexity to the original chart by adding a specific parameter or modifying it, making the decision-making based on the GSI Chart more difficult to find rock strength parameters. In some cases, a rock sample gets a significantly different GSI value for the same outcrop rock. Mixing 3D numerical modeling tools such as synthetic rock mass (SRM) or three-dimensional numerical modeling (3DEC) with GSI values is the most convenient method for estimating joints' strength and assisting engineering geologists in overcoming these obstacles.

DOI: [10.33899/earth.2024.145397.1196](https://doi.org/10.33899/earth.2024.145397.1196), ©Authors, 2025, College of Science, University of Mosul.

This is an open-access article under the CC BY 4.0 license (<http://creativecommons.org/licenses/by/4.0/>).

القياس الكمي لمؤشر القوة الجيولوجية (GSI): مراجعة

فهمي عصمان محمد¹ ID، عزالدين صالح الجوادي^{2*} ID، إيمان جعفر³ ID، كولن ديفي⁴ ID

¹ قسم علوم الأرض، كلية العلوم، جامعة السليمانية، السليمانية، العراق.

² قسم هندسة التعدين، كلية هندسة النفط والتعدين، جامعة الموصل، الموصل، العراق.

³ قسم الجيولوجيا، كلية العلوم، جامعة البصرة، البصرة، العراق.

⁴ كلية الهندسة المدنية وعلوم الأرض، جامعة نيوكاسل، المملكة المتحدة.

المخلص	معلومات الارشفة
تم اختراع مخطط لمؤشر القوة الجيولوجية (GSI) لأول مرة لتصنيف خصائص الكتلة الصخرية. يفترض مطور مخطط GSI أن الجيولوجيين المؤهلين والمهرة أو الجيولوجيين الهندسيين سيقومون بتقييم وتسجيل خصائص الكتلة الصخرية. وبدون خلفية جيولوجية قوية وخبرة ميدانية، فإن العديد من الباحثين يسيئون استخدام مخططات GSI. نظرًا للزيادة غير الطبيعية في مخططات GSI المستخدمة في العقد الأخير، كان التحديث ضروريًا للتخلص من مشكلات التصور والافتراض في مخططات GSI. كان الارتباط بين مخططات GSI الكمية عادةً لتقليل عدم اليقين في تقدير خصائص قوة الصخور. تم تطوير أو تحديث العديد من مخططات GSI ليتم قياسها كميًا بدلاً من المخططات المرئية، والتي أصبحت أكثر تحديدًا وعالمية. تم تعديل مخطط GSI عن طريق إضافة عوامل محددة إلى المخطط الأصلي، مثل حالة الفواصل، وتعيين جودة الصخور RQD، وعدد الفواصل الحجمي، وحجم الكتلة Vb. تسهل مخططات GSI المعدلة الاستخدام العملي بشكل أكبر وتقلل من الأخطاء. ومع ذلك، فإن المراقبة الميدانية والتصوير لا تزال ضرورية لتقدير خاصية قوة الصخور، وخاصة في التصنيف الجيوميكانيكي للكتلة الصخرية. تضيف بعض التعديلات الكثير من التعقيد إلى المخطط الأصلي عن طريق إضافة عامل معين أو تعديله، مما يجعل اتخاذ القرار بناءً على مخطط GSI أكثر صعوبة للعثور على عامل قوة الصخور. في بعض الحالات، تحصل عينة الصخور على قيمة GSI مختلفة تمامًا لنفس الصخور المنكشفة. يعد خلط أدوات النمذجة العددية ثلاثية الأبعاد مثل كتلة الصخور الاصطناعية SRM أو النمذجة العددية ثلاثية الأبعاد 3DEC مع قيمة GSI هي الطريقة الأكثر ملاءمة لتقدير قوة الفواصل ومساعدة الجيولوجيين الهندسيين في التغلب على هذه العوائق.	<p>تاريخ الاستلام: 24- فبراير-2024</p> <p>تاريخ المراجعة: 25- ابريل-2024</p> <p>تاريخ القبول: 11- مايو-2024</p> <p>تاريخ النشر الإلكتروني: 01- ابريل-2025</p> <p>الكلمات المفتاحية:</p> <p>مؤشر القوة الجيولوجية</p> <p>تصنيف جودة الصخور</p> <p>حجم الكتلة</p> <p>الانقطاعات</p> <p>تصنيف كتلة الصخور</p> <p>المراسلة:</p> <p>الاسم: عزالدين صالح الجوادي</p> <p>Email: azealdeenaljwadi@uomosul.edu.iq</p>

DOI: [10.33899/earth.2024.145397.1196](https://doi.org/10.33899/earth.2024.145397.1196), ©Authors, 2025, College of Science, University of Mosul.

This is an open-access article under the CC BY 4.0 license (<http://creativecommons.org/licenses/by/4.0/>).

Introduction

Several geomechanical classifications for rock mass have been developed and updated over the last 50 years to classify and evaluate rock mass properties for specific designs (Table 1), but the GSI chart is the most widely used. For accurate evaluation of a specific rock mass using GSI, experience in rock mass properties together with a geological background are required (Zhang et al., 2019; Hoek and Brown, 2019). However, in many cases, low-skilled engineer staff are chosen to collect data rather than competent field geologist staff and users who ignore the basic knowledge chart of GSI processing (Hoek et al., 2013). The input parameters and the results would be carried out and interpreted by not-qualified individuals with these visual descriptions (Hoek et al., 2013). Recently, the GSI application has been used to approximate different properties of a rock, such as the Representative Elementary Volume (REV) of disintegrated rock masses (Huang et al., 2020) and to describe the weathering conditions of rock failures (Berisavljević et al., 2018). A recent study by Hong et al. (2017) proposed estimating GSI value using satellite images and image processing. Hoek (1994)

introduced GSI to estimate the rock mass characteristics from strong to weak instead of the rock mass rating (RMR) established by Bienawski in 1976 (Abbas and Konietzky, 2017). The original chart employs two parameters, blockiness and surface conditions of discontinuity to assess rock mass (Fig. 1). A higher GSI value indicates a strong blocky and un-weathered surface condition joint, whereas a lower value indicates weak rock, less competent, and heavily weathered jointed rock mass (Marions and Carter, 2018). The GSI chart also filled a gap in RMR for weak rocks rating less than 18 for (RMR1976) or less than 23 for (RMR1986) (Song et al., 2020). Later, the GSI chart went through many modifications to evaluate soft, foliated, laminated, and sheared rocks (Hussain et al., 2020; Osgoui et al., 2010). There is a GSI chart for weak and very weak rocks in case that rock behaves like homogeneous (Hoek et al., 2005), and the GSI chart for molasses and flysch rocks due to the extreme attention necessary for these kinds of rocks. The modified GSI chart for molasses and flysch rock helps to classify quantitatively these rock masses and provides numerical values for engineering design (Marions, 2010). The basic GSI chart (Fig. 1) was used for rating limits to describe the joint surface condition and structure of rock masses and the rating value for each rock category. A cubic rock structure with a very favorable surface condition of discontinuity (B/VG) has a GSI value of less than 85, but greater than 63. All modifications to GSI charts focused on quantifying rock mass units with a unique value (Wu et al., 2018). The results from these modified charts were significantly different and not exact (Bertuzzi et al., 2016; Vásárhelyi et al., 2016). Additionally, intense care about the geology and mechanical condition of the site shows either a small or high value of GSI (Hoek and Brown, 2019). Finally, the GSI chart cannot be applied to structurally controlled failures or transported soil (Hoek et al., 2013).

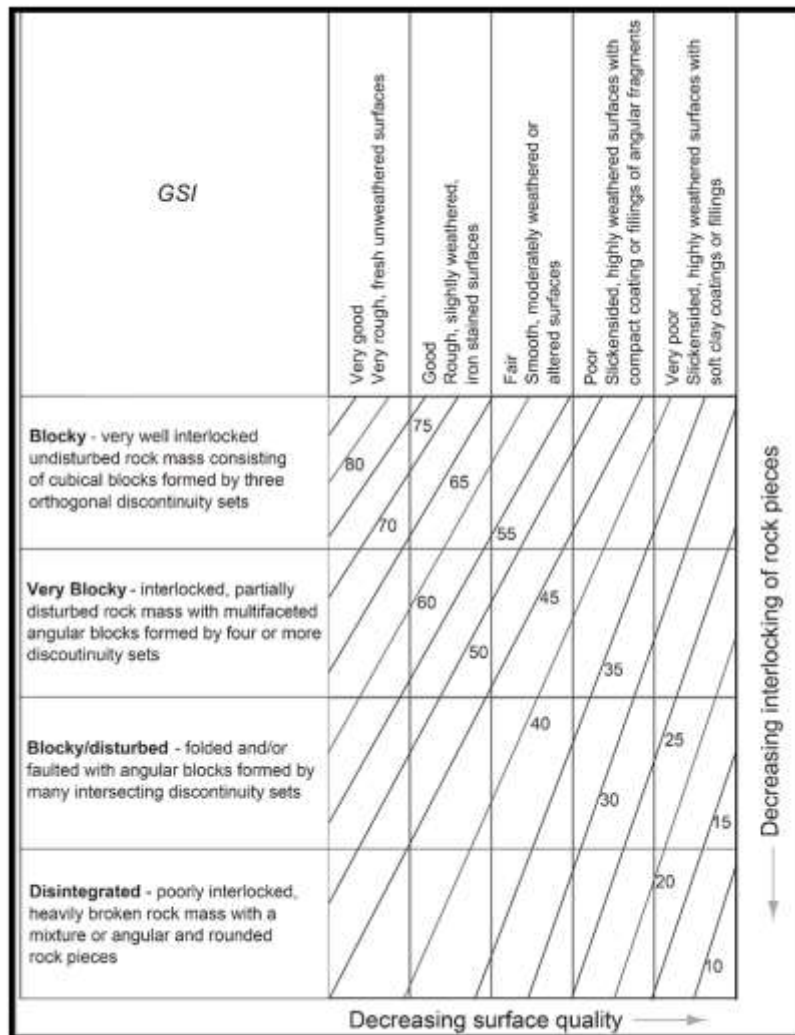


Fig. 1. The initial GSI chart (Hoek and Brown, 1997).

Table 1: The more interesting five rock mass classification system.

No	System	year	Author
1	(RMR) rock mass rating	1976	Tomas et al., 2012
2	(Q-system) rock mass quality system	1974	Ji et al., 2019
3	(RMS) rock mass strength	1982	Kulatilake et al., 2016
4	SMR slope mass rating	1982	Hamasur et al., 2020
5	(RMi) rock mass index	1996	Khamehchiyan et al., 2014

Methodology

The GSI System underwent numerous modifications, and many parameters were added to the axial and horizontal axes of the initial GSI chart to simplify and quantify them. Three joint conditions of Surface Condition Rating (SCR) properties were added as input parameters in the horizontal axis including joint roughness (R_r), joint weathering condition (R_w), and infilling material (R_f) (Tomas et al., 2012). The volumetric joint count (J_v) is added to the vertical axis because this parameter can easily be interpreted visually in the field (Tomas et al., 2012). According to RMR1986, the GSI chart was modified to determine identified values. The Structure Rating (S_R) value is added to the axial axis of the GSI chart to indicate Joint Blockiness (J_v). The original GSI chart requires numerical approaches, but quantitative scales should not limit its use because the GSI chart was designed for ease of use and visual field assessments (Zhang et al., 2019; Hoek et al., 2013; and Cai et al., 2014). In some instances, scaling rock size established on rock quality designation (RQD), (J_v), and quantification of the condition of the joint surface complicates the original GSI. The RQD is used in most classification systems, and it is discovered by logging the core in boreholes; it is sometimes estimated on a rock outcrop by logging the spacing of the discontinuities (Al-Jawadi et al., 2023). The modified charts try to balance the visual interpretation at sites and numerical approaches because rock mass is not always homogeneous, and it contains different rock units with different thicknesses, and each unit must be quantified with its unique values.

Many researchers simplify and quantify the original GSI charts by changing or adding parameters to the vertical and horizontal axes. Sonmez and Ulusay (1999, 2002) suggested and presented simple quantitative parameters based on Bieniaweski's (1989) RMR classification. The newly defined parameters, Structure Rating (S_R) and Surface Condition Rating (SCR) were linked to joint properties and incorporated into the current GSI classification scheme (Hoek and Brown, 1997) (Fig. 2).

Three joint conditions (SCR) properties based on Tomas et al. (2012) are taken as input parameters in the horizontal axis including joint roughness (R_r), Weathering Condition Joint (R_w), Infilling Material (R_f), and (J_v) to vertical axes because these two parameters can easily be interpreted visually in the field. According to RMR (1986), the GSI chart was modified for estimating quantified values. The (S_R) value is applied to the axial axis of the GSI chart to represent (J_v).

SCR value is calculated using equation (1):

$$SCR = R_r + R_w + R_f \dots\dots\dots (1)$$

The maximum value of SCR is 18, which is the total of the six maximum values for weathering, roughness, and infilling material. The horizontal axis is divided into 18 equal parts based on the SCR value as illustrated in Figure (2). Equations (2 and 3) are used to estimate the (J_v) from joint spacing and joint set numbers.

$$Jv = \frac{N1}{L1} + \frac{N2}{L2} + \frac{N3}{L3} + \dots\dots + \frac{Nn}{Ln} + \frac{Nr}{Lr} \dots\dots\dots (2)$$

$$Jv = \frac{1}{s1} + \frac{2}{s2} + \frac{3}{s3} + \dots\dots + \frac{n}{sn} + \frac{r}{sr} \dots\dots\dots (3)$$

where: S is the spacing of the discontinuities; N is the number of discontinuities along the scanline; L is the scanline length; n is the discontinuity set number; r is the random discontinuity set number.

It is difficult to determine discontinuities in all directions during a scanline survey; so, for simplicity, the homogeneous substance assumption of rock mass is used in equation (4).

$$Jv = \left(\frac{N}{L}\right)^3 \dots\dots\dots (4)$$

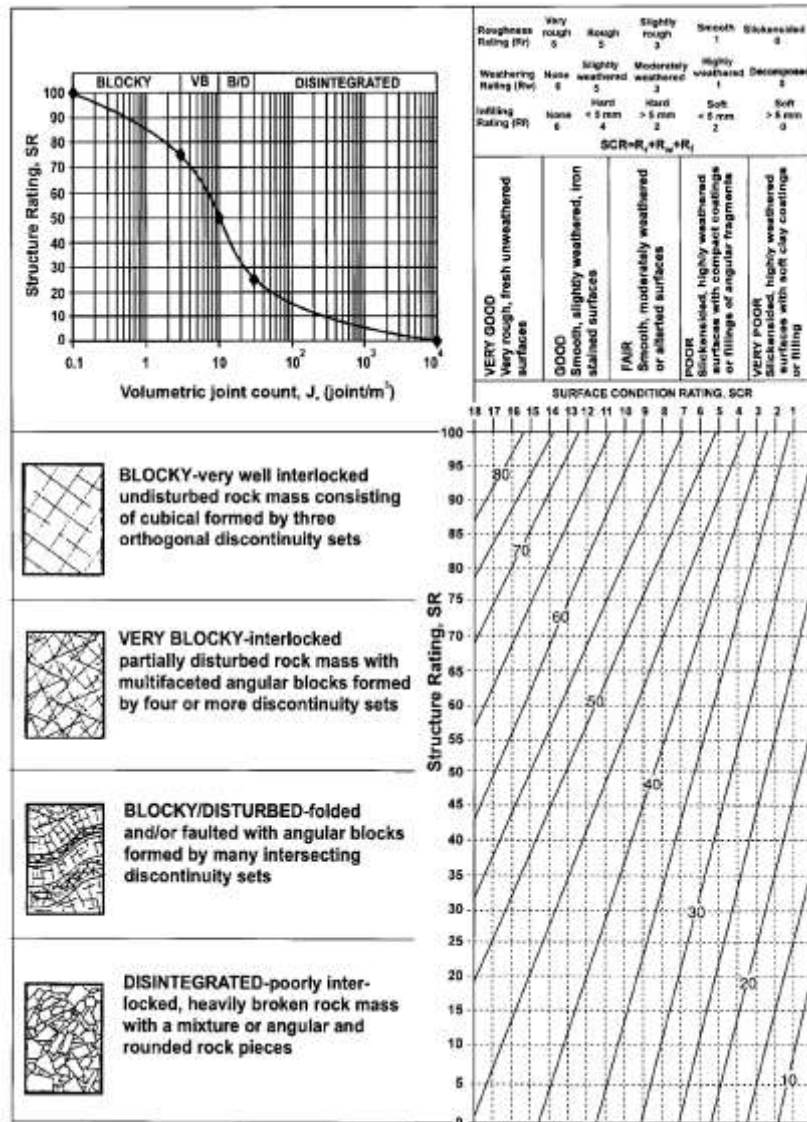


Fig. 2. The modified chart of GSI (Sonmez and Ulusay, 2002).

The factors (Vb and the discontinuity surface condition, Jc) serve as measurable classification parameters (Cai et al., 2004). The (Vb) complements the structure description, while the surface condition of the joint (Jc) factor supplements the discontinuity strength condition. The original GSI chart axes were modified and divided into equal interval-based ratings (Vb) and discontinuity conditions (Fig. 4). Equations (5,6, and 7) can be used to calculate (Vb). The (Jc) is calculated using equation (8) (Kulatilake et al., 2016) by rating joint roughness (Ja) estimates based on Table (2) and joint alteration (Ja) (Table 3) depending on weathering and infillings.

$$Vb = \frac{S1*S2*23}{sin\gamma1*sin\gamma2*sin\gamma3} \dots\dots\dots (5)$$

where: S is discontinuity spacing; γ is the angle between discontinuity sets (Fig. 3).

$$Vb = S1 * S2 * S3 \dots\dots\dots (6)$$

$$Vb = \frac{S1 * S2 * S3}{\sqrt{p1 * p2 * p3}} * \frac{1}{\sin\gamma1 * \sin\gamma2 * \sin\gamma3} \dots\dots\dots (7)$$

where: *p* is the persistent discontinuity factor.

$$Jc = \frac{(Js * Jw)}{Ja} \dots\dots\dots (8)$$

where: *Js* is the discontinuity spacing; *Jw*, is the discontinuity roughness; and *Ja* is the discontinuity alteration ratings in modified GSI charts (Fig. 4).

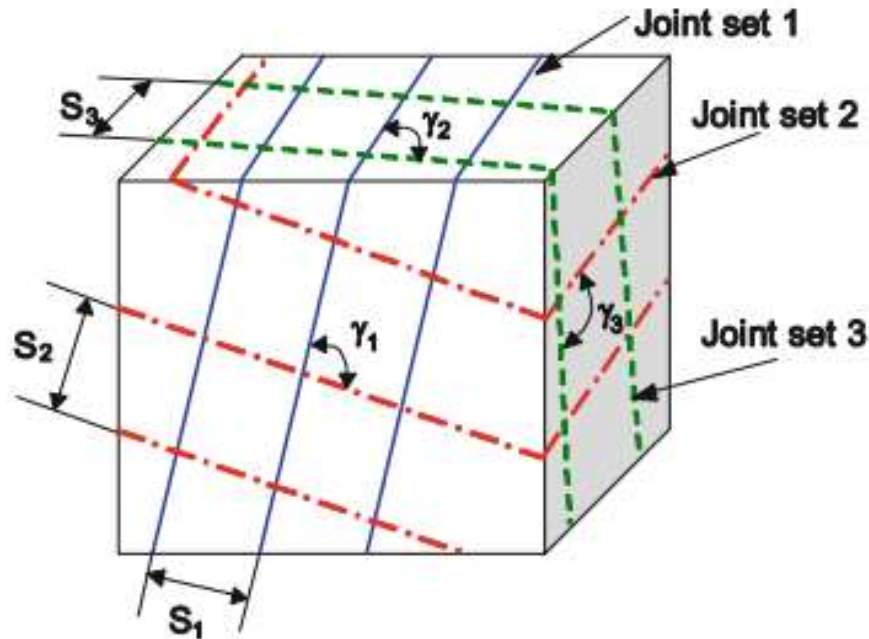


Fig. 3. Angle between discontinuity sets, and discontinuity spacing (Palmstrom, 2005).

The attempt to connect (*Jc*), (*Vb*), and the Rock Mass Index (*RMi*) by Russo (2009) to the original GSI chart, an empirical relation and the Joint Condition Factor (*Cj*) are used (Tiwari *et al.*, 2017). The GSI value for rock mass is estimated using joint parameter (*Jp*) parameters in the *RMi* system resulting in a more rational and unique estimation (Fig. 5), but with a more reliable and applicable range that does not change the original output GSI chart (Russo, 2009). The empirical approach between the *JP* of the *RMi* System and GSI quantifies the interlocked degree of the rock mass strength (σ_{cm}) and the strength of intact rock (σ_c).

$$RMI: \sigma_{cm} = \sigma_c * JP \dots\dots\dots (9)$$

$$GSI = \sigma_{cm} * Sa \dots\dots\dots (10)$$

Where *S* and *a* are constants of the rock mass material (Hoek and Brown, 2019); therefore, for undisturbed rock masses, the *JP* value must equal *Sa*.

$$S = \exp[(GSI - 100)/9] \dots\dots\dots (11)$$

$$a = (0.5) + (0.1666) * \left[\exp\left(-\frac{GSI}{15}\right) - \exp\left(-\frac{20}{3}\right) \right] \dots\dots\dots (12)$$

Then, a straight relationship between both *JP* and GSI may be determined.

$$JP = \exp\left(\frac{GSI - 100}{9}\right) \left(\frac{1}{2}\right) + \left(\frac{1}{6}\right) * \left[\exp\left(-\frac{GSI}{15}\right) - \exp\left(-\frac{20}{3}\right) \right] \dots\dots\dots 13$$

Based on the above relations, a strong rational equation has been improved, and the GSI can be estimated by defining the original one, i.e. including the *JL* factor.

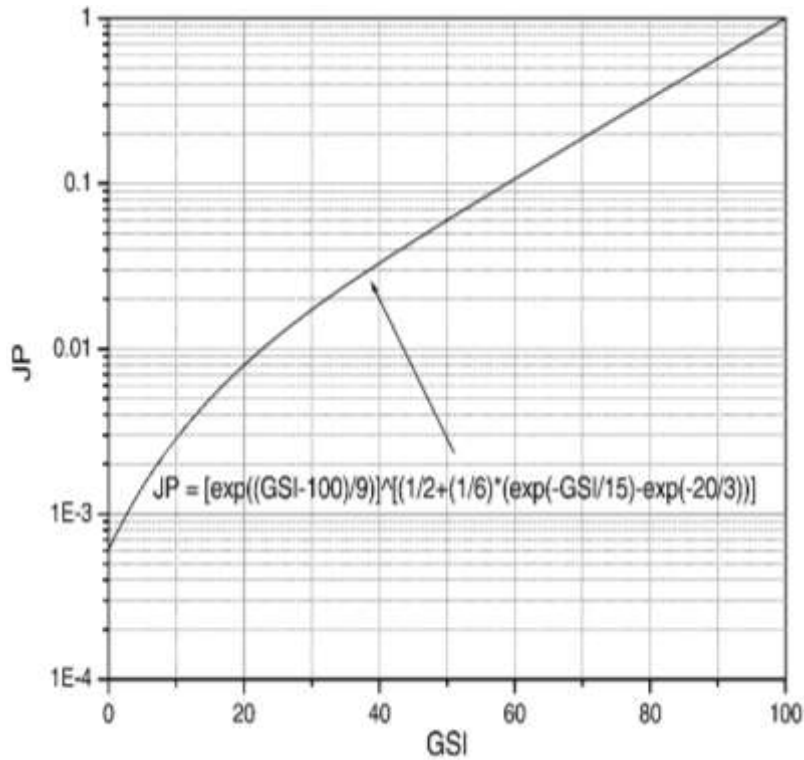


Fig. 5. Relationship between GSI and JP (Russo, 2009).

Table 3: Characterization and rating of (Ja). These values are partially based on Ja in the Q-system (Cai, 2011).

CONTACT BETWEEN THE TWO DISCONTINUITY WALLS			
WALL CHARACTER	DESCRIPTION	jA	
CLEAN DISCONTINUITY S			
-Healed or "welded" discontinuity s	Non-softening, impermeable filling (quartz, epidote, etc.)	0.75	
-Fresh rock walls	No coating or filling on the discontinuity surface, except for staining (rust)	1	
-Alteration of discontinuity wall:			
1 grade more altered	The discontinuity walls show 1 grade of stronger alteration than the rock	2	
2 grades more altered	The discontinuity walls show 2 grades of stronger alteration than the rock	4	
COATING OR THIN FILLING			
-Sand, silt, calcite, etc.	Coating of friction materials without clay	3	
Clay, chlorite, talc, etc.	Coating of softening and cohesive minerals	4	
FILLED DISCONTINUITY WITH PARTLY OR NO WALL CONTACT			
TYPE OF FILLING MATERIAL	DESCRIPTION	Partly wall contact	No wall contact
		thin fillings*) (< approx. 5 mm) jA	thick filling or gouge jA
Sand, silt, calcite, etc	Filling of friction materials without clay	4	8
Compacted clay materials	"Hard" filling of softening and cohesive materials	6	10
Soft clay materials	Medium to low over-consolidation of filling	8	12
Swelling clay materials	Filling material exhibits clear swelling properties	8 - 12	12 - 20

Table 4: The discontinuity size and continuity factor (jL) (Russo, 2009).

LENGTH INTERVAL	TYPE	Discontinuity size factor jL ^{*)}	
		Continuous discontinuity ^a	Discontinuous discontinuity s
0.5	crack	4	8
< 1 m	bedding/foliation partings small	3	6
0.1 - 1.0 m	joint	2	4
1 - 10 m	medium joint	1	2
10 - 30 m	long/large joint	0.75	1.5
> 30 m	very long/large joint/seam ^b	0.5	1

a Discontinuous joints end in massive rock.

b Often a singular discontinuity with significant impact should in these cases be evaluated separately

Hoek et al. (2013) used RQD and Discontinuity Condition parameters that are well-known to quantify GSI charts. Two parameters are used to measure (Vb) and (Jc). These ratings are widely used in engineering design structures because it is easy to calculate. This rating indicates the most significant degree of consistency among various specialties working on a single project. Hoek et al. (2013) expanded the GSI chart of Hoek and Marinos' (2000) by adding scale axes (x and y) represented by (A) and (B). The x-axis (A) represents the surface quality of discontinuity in the rock mass that ranges from 0 to 45 and is divided into five divisions at intervals of nine. The y-axis (B) represents the (Vb), which ranges from 0 to 50 and is divided into five equal divisions at intervals of ten. Hoek et al. (2013) defined in equation (15) the scale (A) as 1.5 J Cond 89, while scale (B) is distinct as RQD/2 in the basic chart of GSI (Fig. 6). This modification's main point is to connect with other rock mass classification, which can help better rock qualification by GSI in equation (14). The joint condition JCond89 value is found in Table (5).

$$GSI = 1.5 * JCond89 + RQD/2 \dots\dots\dots (14)$$

Hoek et al. (2013) also proposed a second method for counting GSI according to the Q System (Barton et al., 1974), which is dependent on (Jr) and frictional characteristics of the filling materials or (ja) corresponds to the equation (15).

$$GSI = \left(\frac{52 \left(\frac{jr}{ja} \right)}{1 + \left(\frac{jr}{ja} \right)} \right) + RQD/2 \dots\dots\dots (15)$$

Morelli (2017) added five alternate parameter scales to the original GSI chart to measure the horizontal and vertical axes. The chart focuses on typical rock mass properties that have been measured to assess rock mass properties. Morelli (2017) included parameters commonly used to describe the structure of rock masses (e.g. Jv, joint spacing S, and RQD/Jn block size factor). The parameters were added as scaled vertical lines to the right side of the GSI chart (Fig. 7).

Table 5: Definition of JCond89 (after Bieniawski, 1989).

Condition of discontinuities	Very rough surfaces Not continuous No separation Unweathered wall rock	Slightly rough surfaces Separation < 1 mm Slightly weathered walls	Slightly rough surfaces Separation < 1 mm Highly weathered walls	Slickensided surfaces or Gouge < 5 mm thick or Separation 1 – 5 mm Continuous	Soft gouge > 5 mm thick or Separation > 5 mm Continuous
Rating	30	25	20	10	0
Guidelines for classification of discontinuity conditions					
Discontinuity length (persistence) Rating	< 1 m 6	1 to 3 m 4	3 to 10 m 2	10 to 20 m 1	More than 20 m 0
Separation (aperture) Rating	None 6	< 0.1 mm 5	0.1 – 1.0 mm 4	1 – 5 mm 1	More than 5 mm 0
Roughness Rating	Very rough 6	Rough 5	Slightly rough 3	Smooth 1	Slickensided 0
Infilling (gouge) Rating	None 6	Hard infilling < 5 mm 4	Hard filling > 5 mm 2	Soft infilling < 5mm 2	Soft infilling > 5mm 0
Weathering Rating	Unweathered 6	Slightly weathered 5	Moderate weathering 3	Highly weathered 1	Decomposed 0

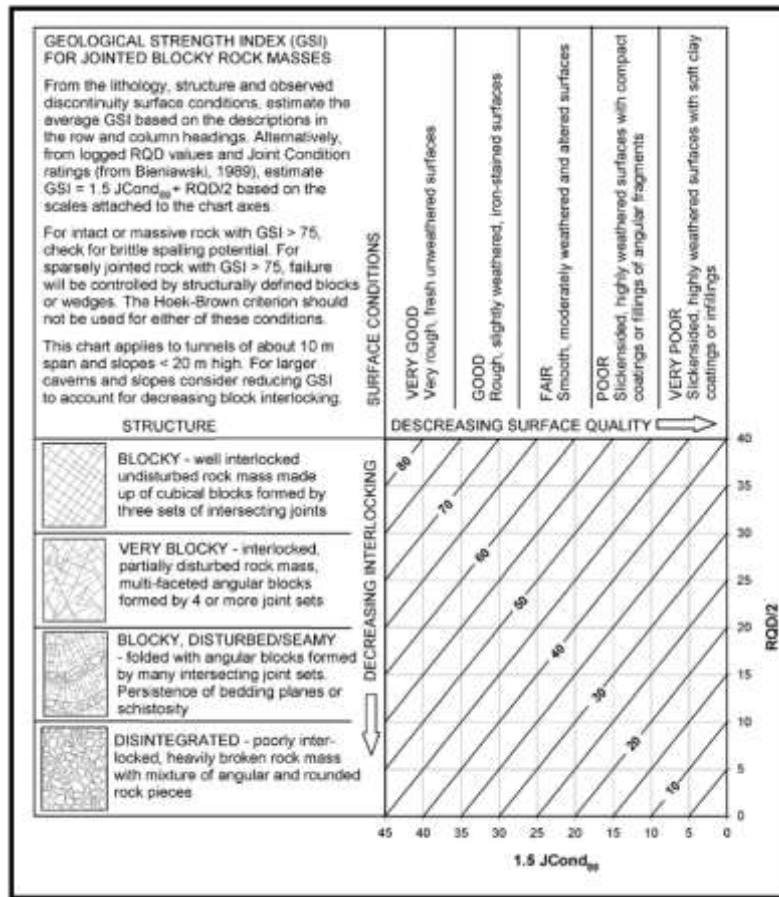


Fig. 6. Modified GSI chart (Hoek et al., 2013).

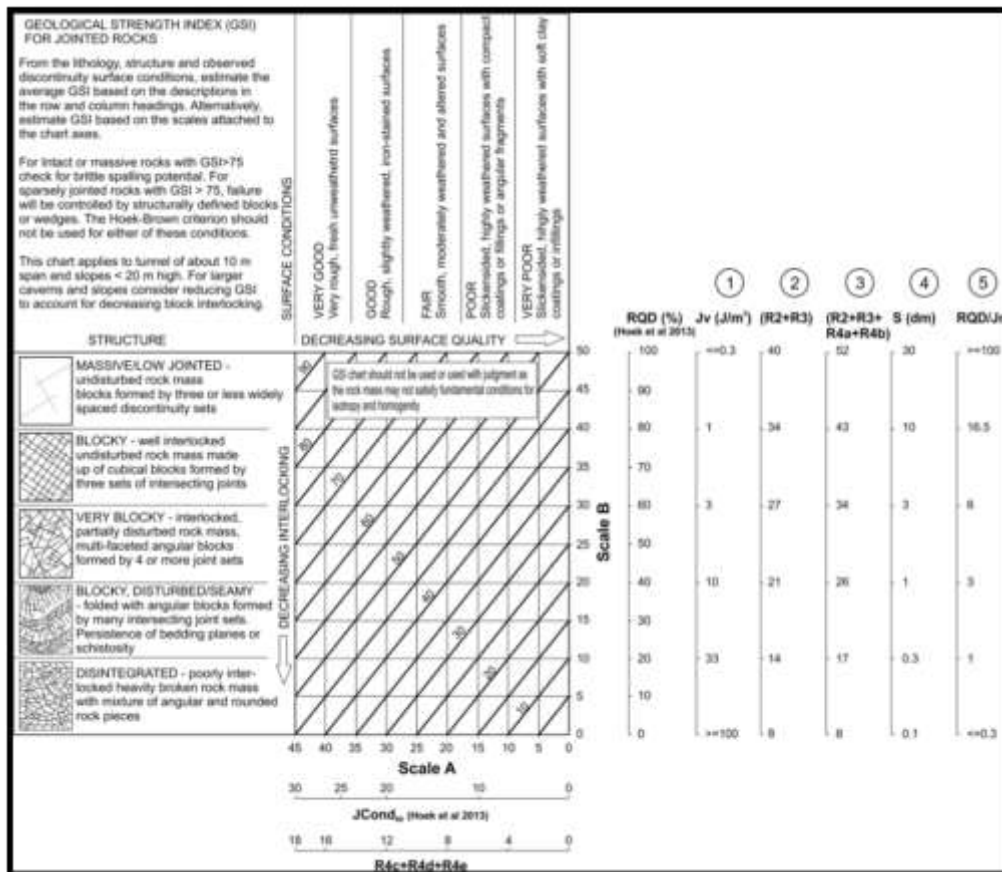


Fig. 7. New quantification scales for the GSI chart (Morelli, 2017).

Discussion

The comparison between rock mass geomechanical classification based on the GSI system and rock mass classification systems helps inexperienced engineers to use it in the field more straightforwardly for different kinds such as flysch, molasses, and massive rocks (Al-Jawadi et al., 2020). The GSI chart qualification gives more simplicity, uniformity, and speed to the geotechnical engineer. The point of weakness quantifies that GSI charts cannot be used for structurally controlled slopes like wedge and toppling or soil (Sardana et al., 2019).

Sonmez and Ulusay (1999, 2002) added two parameters: Block Size and Joint Surface Condition (SCR). The SCR value does not reflect the actual value of (RMRb) (Bieniawski, 1976). According to Tomas et al. (2012), the rating value of SCR is between 15 and 0, not 18 to 0. Cai et al. (2004), and Sonmez and Ulusay (2002) assumed a (J_v) of 1m^3 as a limit between massive and blocky rock masses, but a J_v is the value of 1 joint/ m^3 . This value of J_v ($J_v=1$ joint/ m^3) resembles a (V_b) of 27m^3 , which is incorrect because if J_v equals 1 joint/ m^3 for a limit between blocky and massive rock masses, the V_b can be then calculated using the steps (from a to f) below:

- a. $V_b = \beta j_v - 3$,
- b. $\beta = 20 + 21(S_{max}/S_{min} * n_j)$,
- c. $\beta = 20 + 21(1\text{m}/1\text{m}^3)$, So $\beta = 27$
- d. $J_v = 3$,
- e. $V_b = 27 * (1/3^3) \text{m}^3$
- f. $V_b = 27 \text{m}^3$

Cai et al. (2004) also attempted to estimate (V_b) using the relation between discontinuity spaces. Estimating the discontinuity space of joint sets and random joints is difficult as shown in Figure (4). The field observation is more complicated than an ideal case; sometimes, the joint sets are not transparent or eroded. The geologist must care about the relationship between joint sets and which set is more effective than others. Hamasur (2009) tried to modify the GSI chart based on (Bieniawski 1976, Hoek 1999, and Marion and Hoek 2000) by rating joint surface conditions from 15 to 0. Hamasur (2009) also categorized the rock mass into five categories based on an empirical equation that gives a unique value for categorized (V_b). The (V_b) (Sonmez and Ulusay, 1999; Russo, 2009; and Hamasur, 2009), and rock quality designation (RQD) (Hoek et al., 2013) were added to the vertical axis original GSI chart (Marions and Hoek, 2001). The two parameters (V_b and RQD) give the same block size approaches because the RQD is also calculated based on the block size from the borehole, and (V_b) is calculated based on the relation between joint size, which controls the size of the block pieces in RQD. However, the main difference between the RQD and V_b is that the V_b can be easily found from the outcrop while the RQD needs drilled borehole (BH) or Scanline (SL) of well-preserved outcrop rocks. The blockiness, RQD, and V_b are the main points of modification in the last 20 years, which suffer from the problems related to the size of the block, block direction, and structurally controlled tunnel and slope; therefore, the selection of the GSI chart for evaluating slope and tunnel is not a correct or not a good choice. To reduce the effect of block direction and structurally controlled tunnel and slope, Cai et al. (2004) and Hoek et al. (2013) added joint conditions for horizontal axes based on the (Cai, 2011; Fekete and Diederichs, 2013) classifications for the condition of the joint, which represents the strength properties. Zhang et al. (2019) quantified GSI and RMR by focusing on the intact rock uniaxial compressive strength (UCS), though this correlation is only valid for GSI values greater than twenty and less than 80. Morelli (2017) suggested a more complicated chart based on Hoek et al. (2013), that the simplicity of using the GSI chart was neglected. Vásárhelyi et al. (2016) and Yang et al. (2021) concluded that the modified GSI chart is not exact and contains significant differences. The result should be treated very well. Some modifications added ambiguity by adding a specific parameter, which made the decision-making based on the GSI chart harder.

Conclusion

The geomechanical classification based on GSI lacks three main factors: stress condition, groundwater condition, and blast damage. These three factors are critical to evaluating the rock mass for any project. The mixing processes of GSI chart values with Q-system or Q-slope will help assess stress conditions for rock mass tunnels and slopes, and mixing GSI charts with RMI will help in assessing the effect of joint strength, joint size, and joint length for foundations. Depending on the situation of the rock mass at the location, a different version of GSI charts modified from the original GSI chart must be used, but the final decision is based on visual interpretation, which must be done by very well-trained engineering geologists on-site. A rock mass joint survey is more important than the choice of modified GSI charts at the site. Mixing the 3D numerical model tools such as synthetic rock mass or three-dimensional numerical modeling (3DEC) with GSI value is the most convenient method for estimating joints' strength and assisting engineering geologists in overcoming these obstacles.

References

- Abbas, S.M. and Konietzky, H., 2017. Rock Mass Classification Systems, Introduction to Geomechanics, Vol. 9, No. 2017, pp. 1-48.
- Al-Jawadi, A.S., Abdul Baqi, Y.T., and Sulaiman, A.M., 2020. Qualifying the Geotechnical and Hydrological Characteristic of the Bandawaya Stream Valley-Northern Iraq, *Scientific Review – Engineering and Environmental Sciences*, 29 (3), pp. 319-331, DOI: <https://10.22630/PNIKS.2020.29.3.27>.
- Al-Jawadi, A.S., Al-Jumaily, I.S., Al-Dabbagh, Th. H. and Davie, C., 2023. Evaluation of the Bekhme Dam Site – NE Iraq Using the Proposed Reduction System of the Rock Mass Strength, *Iraqi National Journal of Earth Science*, Vol. 23, No. 1, pp. 85-106, <https://doi:10.33899/earth.2023.137501.1036>
- Berisavljević, Z., Berisavljević, D., Rakić, D. and Radić, Z., 2018. Application of Geological Strength Index for Characterization of Weathering-Induced Failures, *Građevinar*, Vol. 70, No. 10, pp. 891-903, <https://doi:10.14256/JCE.1876.2016>.
- Bertuzzi, R., Douglas, K. and Mostyn, G., 2016. Comparison of Quantified and Chart GSI for Four Rock Masses, *Engineering Geology*, Vol. 202, pp. 24-35, <http://dx.doi.org/10.1016/j.enggeo.2016.01.002>.
- Bieniawski, Z.T., 1976, Rock Mass Classifications in Rock Engineering, Proceeding Symposium on Exploration for Rock Engineering, Johannesburg, ed. Bieniawski publ., Balkema, Rotterdam, pp. 97-106.
- Cai, M., 2011. Rock Mass Characterization and Rock Property Variability Considerations for Tunnel and Cavern Design, *Rock mechanics and rock engineering*, Vol. 44, No. 4, pp. 379-399, <https://doi.org/10.1007/s00603-011-0138-5>.
- Cai, M., Kaiser, P.K., Uno, H., Tasaka, Y. and Minami, M., 2004. Estimation of Rock Mass Deformation Modulus and Strength of Jointed Hard Rock Masses Using the GSI System, *International Journal of Rock Mechanics and Mining Sciences*, Vol. 41, No. 1, pp. 3-19, [https://doi:10.1016/S1365-1609\(03\)00025-X](https://doi:10.1016/S1365-1609(03)00025-X).
- Fekete, S. and Diederichs, M., 2013. Integration of Three-Dimensional Laser Scanning with Discontinuum Modelling for Stability Analysis of Tunnels in Blocky Rock Masses, *International Journal of Rock Mechanics and Mining Sciences*, Vol. 57, pp. 11-23, <https://doi.org/10.1016/j.ijrmms.2012.08.003>.
- Hamasur G.A., 2009. Rock Mass Engineering of The Proposed Basara Dam Site, Sulaimani, Kurdistan Region, NE-Iraq, Ph.D. Thesis, University of Sulaymaniyah, Iraq.

- Hamasur, G.A., Mohammed, F.O. and Ahmad, A.J., 2020. Assessment of Rock Slope Stability along Sulaimaniyah-Qaradagh Main Road, Near Dararash Village, Sulaimaniyah, NE-Iraq, *Iraqi Journal of Science*, pp. 3266–3286, Dec. 2020, <https://doi.org/10.24996/ij.s.2020.61.12.15>.
- Hoek, E., 1999. Putting Numbers to Geology – An Engineer’s Viewpoint, *Quarterly Journal of Engineering Geology*, Vol. 32, No. 1, 1999, pp. 1-19, <https://doi.org/10.1144/GSL.QJEG.1999.032.P1.01>.
- Hoek, E. and Brown, E.T., 1997. Practical Estimates of Rock Mass Strength, *International journal of rock mechanics and mining sciences*, Vol. 34, No. 8, pp. 1165–1186, [https://doi.org/10.1016/S1365-1609\(97\)80069-X](https://doi.org/10.1016/S1365-1609(97)80069-X).
- Hoek, E. and Brown, E.T., 2019. The Hoek–Brown Failure Criterion and GSI–2018 Edition, *Journal of Rock Mechanics and Geotechnical Engineering*, Vol. 11, No. 3, pp. 445-463, <https://doi.org/10.1016/j.jrmge.2018.08.001>.
- Hoek, E., Carter, T. G. and Diederichs, M. S., 2013. Quantification of the Geological Strength Index Chart, American Rock Mechanics Association, 47th US Rock Mechanics/ Geomechanics Symposium held in San Francisco, CA, USA, 23-26 June 2013, 8P.
- Hoek, E., Marinos, P.G. and Marinos, V.P., 2005. Characterisation and Engineering Properties of Tectonically Undisturbed but Lithologically Varied Sedimentary Rock Masses, *International Journal of Rock Mechanics and Mining Sciences*, Vol. 42, No. 2, pp. 277-285, <https://doi.org/10.1016/j.ijrmms.2004.09.015>.
- Hong, K., Han, E. and Kang, K., 2017. Determination of Geological Strength Index of Jointed Rock Mass Based on Image Processing, *Journal of Rock Mechanics and Geotechnical Engineering*, Vol. 9, No. 4, pp. 702-708, <https://doi.org/10.1016/j.jrmge.2017.05.001>.
- Huang, H., Shen, J., Chen, Q. and Karakus, M., 2020. Estimation of REV for Fractured Rock Masses Based on Geological Strength Index, *International Journal of Rock Mechanics and Mining Sciences*, Vol. 126, pp. 104179, <https://doi.org/10.1016/j.ijrmms.2019.104179>.
- Hussian S., Mohammad, N., Rehman, Z.U., Khan, N.M., Shahzada, K., Ali, S., Tahir, M., Raza, S. and Sherin, S., 2020. Review of the Geological Strength Index (GSI) as an empirical classification and rock mass property estimation tool: origination, modifications, applications, and limitations, *Advances in Civil Engineering*, Vol. 2020, <https://doi.org/10.1155/2020/6471837>.
- Ji, F., Shi, Y., Li, R., Zhou, C., Zhang, N. and Gao, J., 2019. Modified Q-index for Prediction of Rock Mass Quality Around a Tunnel Excavated with a Tunnel Boring Machine (TBM), *Bulletin of Engineering Geology and the Environment*, Vol. 78, No. 5, pp. 3755-3766, <https://doi.org/10.1007/s10064-018-1257-y>.
- Khamehchiyan, M., Rahimi Dizadji, M. and Esmaeili, M., 2014. Application of Rock Mass Index (RMI) to the Rock Mass Excavatability Assessment in Open Face Excavations, *Geomechanics and Geoengineering*, Vol. 9, No. 1, pp. 63-71, <https://doi.org/10.1080/17486025.2013.806996>.
- Kulatilake, P.H.S.W., Shreedharan, S., Sherizadeh, T., Shu, B., Xing, Y. and He, P., 2016. Laboratory Estimation of Rock Joint Stiffness and Frictional Parameters, *Geotechnical and Geological Engineering*, Vol. 34, No. 6, pp. 1723-1735, <https://doi.org/10.1007/s10706-016-9984-y>.
- Marinos, P. and Hoek, E., 2000. GSI: A Geologically Friendly Tool for Rock Mass Strength Estimation, Paper presented at the ISRM International Symposium, Melbourne, Australia, November 2000.

- Marinos, P. and Hoek, E., 2001. Estimating the Geotechnical Properties of Heterogeneous Rock Masses such as Flysch, *Bull Eng Geol Environ*, Vol. 60, No. 2, pp. 85-92, [https://doi:10.1007/s100640000090](https://doi.org/10.1007/s100640000090).
- Marinos, P.V., 2010. New Proposed GSI Classification Charts for Weak or Complex Rock Masses, *Bulletin of the Geological Society of Greece, Proceedings of the 12th International Congress*, Vol. 43, No. 3, pp. 1248-1258.
- Marinos, V. and Carter, T.G., 2018. Maintaining Geological Reality in the Application of GSI for the Design of Engineering Structures in Rock, *Engineering Geology*, Vol. 239, pp. 282-297, <https://doi.org/10.1016/j.enggeo.2018.03.022>.
- Morelli, G.L., 2017. Alternative Quantification of the Geological Strength Index Chart for Jointed Rocks, *Geotechnical and Geological Engineering*, Vol. 35, No. 6, pp. 2803-2816, <https://doi.org/10.1007/s10706-017-0279-8>.
- Osgoui, R.R., Ulusay, R. and Unal, E., 2010. An Assistant Tool for the Geological Strength Index to Better Characterize Poor and Very Poor Rock Masses, *International Journal of Rock Mechanics and Mining Sciences*, Vol. 47, No. 4, pp. 690-697, <https://doi.org/10.1016/j.ijrmms.2010.04.001>.
- Palmstrom, A., 2005. Measurements of and Correlations Between Block Size and Rock Quality Designation (RQD), *Tunnelling and Underground Space Technology*, Vol. 20, No. 4, pp. 362-377, <https://doi.org/10.1016/j.tust.2005.01.005>.
- Russo, G., 2009. A New Rational Method for Calculating the GSI, *Tunnelling and Underground Space Technology*, Vol. 24, No. 1, pp. 103-111, <https://doi.org/10.1016/j.tust.2008.03.002>.
- Sardana, S., Verma, A.K., Verma, R. and Singh, T.N., 2019. Rock Slope Stability Along Road Cut of Kulikawn to Saikhamakawn of Aizawl, Mizoram, India, *Nat Hazards*, Vol. 99, No. 2, pp. 753-767, <https://doi.org/10.1007/s11069-019-03772-4>.
- Song, Y., Xue, H. and Ju, G., 2020. Comparison of Different Approaches and Development of Improved Formulas for Estimating GSI, *Bulletin of Engineering Geology and the Environment*, Vol. 79, No. 6, pp. 3105-3119, <https://doi.org/10.1007/s10064-020-01739-5>.
- Sonmez, H. and Ulusay, R., 1999. Modifications to the Geological Strength Index (GSI) and Their Applicability to Stability of Slopes, *International Journal of Rock Mechanics and Mining Sciences*, Vol. 36, No. 6, pp. 743-760, [https://doi.org/10.1016/S0148-9062\(99\)00043-1](https://doi.org/10.1016/S0148-9062(99)00043-1).
- Sonmez, H. and Ulusay, R., 2002. A Discussion on the Hoek-Brown Failure Criterion and Suggested Modifications to the Criterion Verified by Slope Stability Case Studies, *Yerbilimleri*, Vol. 26, No. 1, pp. 77-99.
- Tiwari, G., Pandit, B., Latha, G.M. and Babu, G.S., 2017. Probabilistic Analysis of Tunnels Considering Uncertainty in Peak and Post-Peak Strength Parameters, *Tunnelling and Underground Space Technology*, Vol. 70, pp. 375-387, <https://doi.org/10.1016/j.tust.2017.09.013>.
- Tomas, R., Cuenca, A., Cano, M. and García-Barba, J., 2012. A Graphical Approach for Slope Mass Rating (SMR), *Engineering Geology*, Vol. 124, pp. 67-76, <https://doi.org/10.1016/j.enggeo.2011.10.004>.
- Vásárhelyi, B., Somodi, G., Krupa, Á. and Kovács, L., 2016. Determining the Geological Strength Index (GSI) Using Different Methods, *Rock Mechanics and Rock Engineering*:

From the Past to the Future – Ulusay et al. (Eds), Taylor and Francis Group, London, ISBN 978-1-138-03265-1.

- Wu, L., Adoko, A.C. and Li, B., 2018. An Illustration of Determining Quantitatively the Rock Mass Quality Parameters of the Hoek–Brown Failure Criterion, *Rock Mechanics and Rock Engineering*, Vol. 51, No. 4, pp. 1063-1076, <https://doi.org/10.1007/s00603-017-1375-z>.
- Yang, B., Mitelman, A., Elmo, D. and Stead, D., 2021. Why the Future of Rock Mass Classification Systems Requires Revisiting Their Empirical Past, *Quarterly Journal of Engineering Geology and Hydrogeology*, <https://doi.org/10.1144/qjegh2021-039>.
- Zhang, Q. Huang, X. Zhu, H. and Li, J., 2019. Quantitative Assessments of the Correlations Between Rock Mass Rating (RMR) and Geological Strength Index (GSI), *Tunnelling and Underground Space Technology*, Vol. 83, pp. 73-81, <https://doi.org/10.1016/j.tust.2018.09.015>.